

Sun-View Angle Effects on Reflectance Factors of Corn Canopies

K. J. RANSON, C. S. T. DAUGHTRY, L. L. BIEHL, and M. E. BAUER*

Laboratory for Applications of Remote Sensing, Purdue University, West Lafayette, Indiana 47907

The bidirectional reflectance characteristics of vegetation canopies vary with time of day and through the growing season. In this study the effects of sun and view angles on bidirectional reflectance factors from corn (*Zea mays* L.) canopies ranging in development from the six leaf stage to harvest maturity were examined. For nadir-acquired reflectance factors there was a strong solar angle dependence in all spectral bands for canopies with low leaf area index (LAI). A decrease in contrast between bare soil and vegetation due to shadows at larger solar zenith angles appeared to be the cause of this dependence. Sun angle dependence was least for well-developed canopies with higher LAI. However, for higher LAI canopies a moderate increase in reflectance factor was observed at larger solar zenith angles and was attributed to the presence of specular reflectance. Trends of off-nadir reflectance factors with respect to sun angle at different view azimuth angles indicated that the position of the sensor relative to the sun was an important factor for determining the angular reflectance characteristics of corn canopies. Reflectance factors were maximized for coincident sun and view angles and minimized when the sensor view direction was towards the sun. View direction relative to row orientation also contributed to the variation in reflectance factors.

Introduction

The non-Lambertian characteristics of vegetation complicate the analysis of remote sensing data especially when off-nadir view angles are used. Field studies that have examined the directional reflectance of vegetated surfaces (Eaton and Dirmhirn, 1979; Vanderbilt et al., 1980; Kirchner et al., 1982; Guyot, 1983; Kimes, 1983; Ranson et al., 1985) have reported a dependence due to sun angle and view angle.

Such studies are important for the characterization of reflectance distributions with the goal of enhancing the interpretation of remotely sensed data. In addition, the data are useful for validating radiative transfer models designed to predict the reflectance behavior of vegetation canopies (Cooper et al., 1982; Kimes

and Kirchner, 1982; Norman and Welles, 1983; Suits, 1983).

A number of field studies have documented the effects of changing sun angle on vegetation canopy reflectance. Kollenkark et al. (1982) reported large relative changes in reflectance from soybean (*Glycine max* (L.) Merr.) canopies in a red (0.6–0.7 μm) wavelength band as a function of solar zenith and azimuth angles, but observed small relative changes in a near-infrared (0.8–1.1 μm) band. They concluded that the relationship between row direction and solar zenith and azimuth angles was more important for incomplete than complete (or full) vegetation canopies. A general decline in reflectance with increasing solar zenith angle was noted by Colwell (1974), Eaton and Dirmhirn (1979), and Kirchner et al. (1982) for agricultural crops. Smith et al. (1975), however, observed both increasing and decreasing trends of reflectance factors for wheat, depending on the

*Current address: Remote Sensing Laboratory, University of Minnesota, St. Paul, MN 55108.

stage of development. Kimes et al. (1980) summarized the diurnal trends of reflectance from vegetated surfaces and cautioned that the wide variability reported in the literature may be the result of variations in sky irradiance, canopy geometry, and the type of reflectance measurement.

The characterization of reflectance data acquired under a wide variety of sun and view angle conditions is important if the data from sensors with off-nadir viewing capabilities are to be used effectively. This is the case for operational and proposed (Jackson, 1984) aircraft-mounted multispectral scanners and the satellite-mounted Advanced Very High Resolution Radiometer (AVHRR) which has an across-track scan angle of $\pm 56^\circ$ (Schneider and McGinnis, 1982). Other satellite systems with off-nadir viewing capabilities are currently under development with the European SPOT satellite scheduled for launch in 1985 (Chevrel et al., 1981).

In this study, reflectance factors were measured for a corn (*Zea mays* L.) field during the 1982 growing season over a wide range of sun and view angles. The objective was to quantify the variation in diurnal and seasonal reflectance factors at many view angles.

Experiment

The field utilized in this study was located at the Purdue University Agronomy Farm located 10 km northwest of West Lafayette, IN ($40^\circ 28'N$ $86^\circ 59'W$). Corn (*Zea mays* L. "Asgro RX777") was planted in a Chalmers silty clay loam (typic Argiaquoll) soil on 11 May 1982 with an average population density of 62,200 plants/ha in north-south rows [row azimuth (ϕ_r) = 0°] spaced 0.76 m apart. The field was 200×200 m in size and uniform with respect to soil type, drainage, and slope ($< 2\%$). Plant growth and development were uniform throughout the field.

The data collection commenced on 13 June 1982 and continued until 25 October when the field was at harvest maturity. Spectral radiometric data were acquired with a Barnes Model 12-1000 multiband radiometer. This instrument has eight channels sensitive to visible, reflective infrared and thermal infrared radiation as described in Table 1. The instrument was positioned at view zenith angles (θ_v) of 0, 7, 15, 22, 30, 45, 60, and 70° for each view azimuth angle (ϕ_v) of 0 (looking north), 45, 90, 135, 180, 225, 270, and 315° . This set of 64 view zenith and azimuth angle combinations defines a

TABLE 1 Description of Wavelength Bands of Barnes Modular Multiband Radiometer (MMR) and Corresponding Landsat Thematic Mapper Channels^a

MMR BAND	TM BAND	WAVELENGTH (μm)
1	1	0.45-0.52
2	2	0.52-0.60
3	3	0.63-0.69
4	4	0.76-0.90
5	—	1.15-1.30
6	5	1.55-1.75
7	7	2.08-2.35
8	6	10.60-12.50

^aMMR bands 5 and 8 were not used in this analysis.

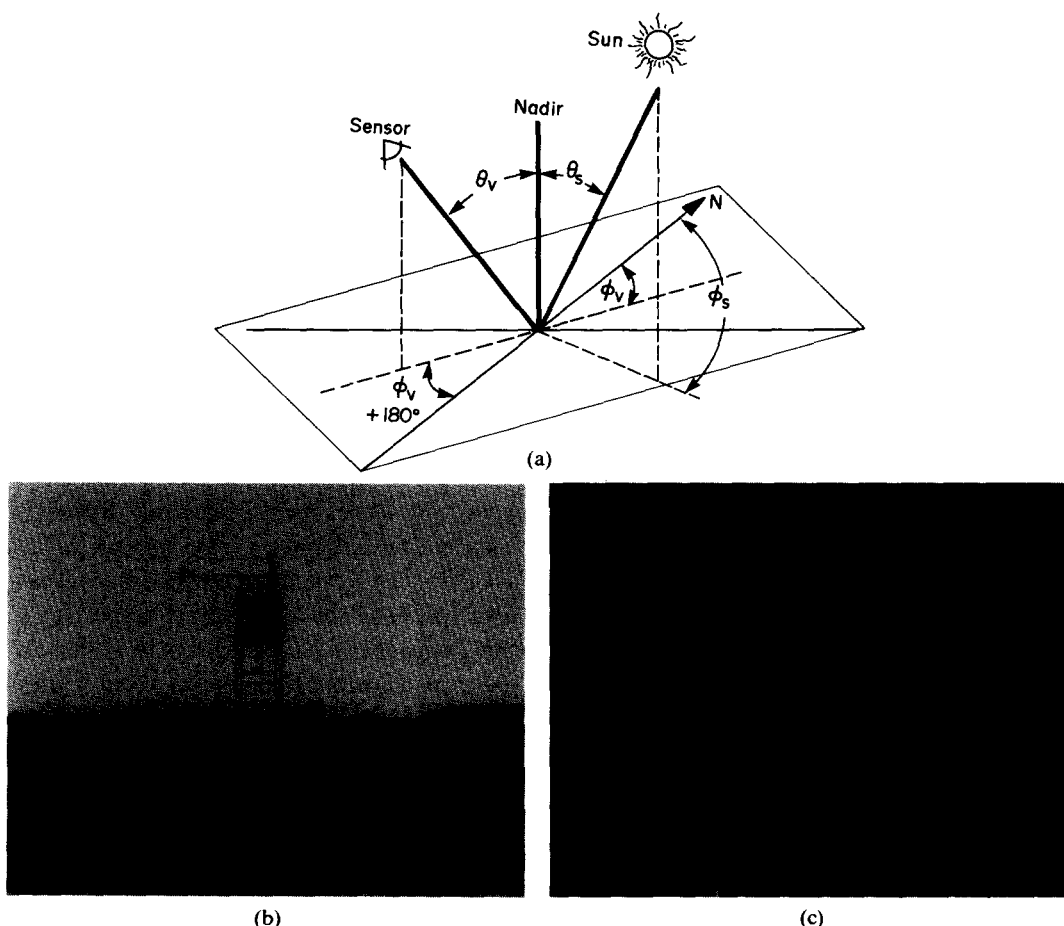


FIGURE 1. (a). Diagram of coordinate system. (b) Tower system. (c) Radiometer and camera mounted on boom pointed off-nadir at 45° .

measurement hemisphere. Measurement hemispheres were obtained at about 1-h intervals to provide varying solar zenith (θ_s) and solar azimuth (ϕ_s) angles. The coordinate system used for the measurements is diagrammed in Fig. 1(a). Spectral data were acquired during 21 days in the summer of 1982 as long as suitable irradiance conditions existed. Six days with extended sun angle ranges were selected for analysis and are summarized in Table 2.

Two methods for acquiring spectral data were employed. During June and

July, data were acquired with a truck-mounted system while in August, September, and October a tower was used. With the truck system, a half hemisphere of data was collected from each side of the field with the radiometer, equipped with 15° field of view stops, looking into the field. From a position on the west side of the field, spectral measurements of a series of view zenith angles were taken at view azimuth angles of 0, 45, 90, 135, and 180° . Reflectance of a bare soil plot located adjacent to the truck was acquired at a nadir view angle. The truck was

TABLE 2 Summary of Solar Zenith and Azimuth Angles During the Times That Spectral Data Were Acquired in 1982^a

DATE	START TIME [CUT (h)]	END TIME	ZENITH (max-min-max) (°)	AZIMUTH (min-max)	NO. DATA SETS	CLOUD COVER (%)
13 June	1724	2158	18-17-55	162-272	9	1-10
24 June	1407	1838	49-18-20	92-214	10	5-10
23 July	1425	2242	49-23-64	98-275	17	1-10
12 Aug.	1408	1915	53-25-31	102-222	24	0-20
4 Sep.	1413	2130	48-33-70	123-262	24	0-1
25 Oct.	1630	2130	53-52-80	170-245	18	10-15

^aTimes are Coordinated Universal Time (CUT) as reported by U.S. National Bureau of Standards station WWV. Subtract 5 h for local time.

moved to the east side of the field and a series of spectral measurements at view zenith angle were made for view azimuths of 0, 180, 225, 270, 315° completing the measurement hemisphere. Several additional spectral measurements of the corn field were acquired at a nadir view angle on the west and east sides of the field.

Prior to and after each half hemisphere of data was collected, spectral measurements were acquired from a barium sulfate (BaSO₄) calibration panel. The data for each wavelength band were calibrated to reflectance factor using

$$RF(\theta_s, \phi_s; \theta_v, \phi_v) = \frac{D_s(t_s)}{D_r(t_1) + [(t_s - t_1)/(t_2 - t_1)] [D_r(t_2) - D_r(t_1)]} \times R_r(\theta_s, \phi_s, 0, 0), \quad (1)$$

where $RF(\theta_s, \phi_s; \theta_v, \phi_v)$ and $R_r(\theta_s, \phi_s; 0, 0)$ are the reflectance factors of the scene and reflectance calibration panel, respectively. $D_s(t_s)$ is the instrument response

(less the dark input response) from the corn canopy at time t_s . $D_r(t_1)$ and $D_r(t_2)$ are the before and after instrument responses (less the dark input response) to the calibration panels. Note that the angles of illumination (θ_s, ϕ_s) and view (θ_v, ϕ_v) for a scene reflectance measurement are defined by the time (t_s). The quantity $R_r(\theta_s, \phi_s; 0, 0)$ adjusts for non-Lambertian properties of the reference panel.

Care was taken to make measurements only when atmospheric conditions did not cause varying illumination conditions for periods of at least 0.5 h. Total shortwave irradiance was measured with a pyranometer (Eppley model 8-18) to document illumination conditions throughout the data collection period. The calibration panel data and pyranometer stripcharts were examined to determine which, if any, data should be discarded because of illumination variations. The collection and calibration of spectral reflectance data adhered to guidelines specified by Robinson and Biehl (1979). A full set of measurements was acquired in less than 0.5 h. To document the field of view (FOV), 35-mm color photographs were obtained for each view position.

A tower was erected in the center of the corn field during the first week of August. The tower was constructed of six 1.5-m sections of scaffolding with platforms mounted on the fifth and top sections [Fig. 1(b)]. The lower platform accommodated data logging equipment. A 3.0 m boom was mounted on a pivot base in the center of the top platform. The boom was inserted into a sleeve and could be rotated about the horizontal axis by means of a wheel attached to one end. The radiometer was attached to the other end of the boom [Fig. 1(c)]. Rotating the boom about its vertical pivot point provided selection of the eight azimuth positions described above. The procedure consisted of selecting a view azimuth angle, setting the view zenith angle at 70° and making successive measurements as the zenith angle was changed to 60, 45, 30, 22, 15, 7, and 0°. Then measurements were made as the view zenith angle was increased until 70° at the opposite view azimuth angle was reached. A complete circuit around the tower resulted in two replications of all eight azimuth angles and all eight zenith angles.

Calibration measurements were made prior to and after each circuit with a BaSO₄ painted panel resting on a platform mounted on the south side of the tower. It was possible to acquire two complete hemispheres of data and calibration measurements in less than 15 min. Due to the number of observations acquired with this system, color photographs documenting the field of view were taken at each view position only a few times each day. Photographs were acquired, however, whenever the instrument operator determined that a tower shadow might fall within the FOV. The FOV was changed to 10° for the tower

system to ensure that the tower sides and immediate ground area were not included in nadir observations.

To facilitate diurnal comparisons, the sun position is represented by the projected solar angle (θ_{sp}). This angle is the zenith angle of the solar vector projected onto a plane perpendicular to the row direction. It is calculated by

$$\theta_{sp} = \left| \tan^{-1} \left[\tan(\theta_s) \sin(\phi_s - \phi_r) \right] \right|, (2)$$

where θ_s = solar zenith angle, ϕ_s = solar azimuth angle, and ϕ_r = row azimuth measured clockwise from north.

The projected solar angle combines the solar zenith and azimuth angles into a single angle projected onto a plane perpendicular to the row direction. Note that ϕ_r for our experiments was 0°. Table 3 presents the solar zenith angles, solar azimuth angles, and times of day for θ_{sp} of 0, 30, and 60° for the six measurement days. For graphical convenience, the angles were arbitrarily assigned negative values for data acquired in the morning and positive values for afternoon data.

Agronomic and geometric measurements describing the canopies were acquired within 3 days of the spectral measurements. These included leaf area index (LAI), total fresh phytomass, stage of development (Ritchie and Hanway, 1982), percent canopy cover, leaf angle distribution (Smith et al., 1977; Ranson, 1983), and leaf spectral reflectance and transmittance measurements. Meteorological data including relative humidity, air temperature, barometric pressure, wind direction, wind speed, and global solar irradiance were also acquired for each measurement day at the Purdue Agronomy Farm.

TABLE 3 Solar Zenith Angles (θ_s), Solar Azimuth Angles (ϕ_s), and Coordinated Universal Times (CUT) for Calculated Projected Solar Angles (θ_{sp})^a

DATE		PROJECTED SOLAR ANGLE (°)				
		- 60	- 30	0	30	60
13 June	θ_s (°)	60	32	17	32	60
	ϕ_s (°)	84	112	180	248	276
	CUT (h)	1305	1535	1744	1955	2223
24 June	θ_s (°)	60	32	17	32	60
	ϕ_s (°)	83	111	180	249	277
	CUT (h)	1307	1536	1746	1956	2226
23 July	θ_s (°)	60	33	20	33	60
	ϕ_s (°)	88	118	180	243	272
	CUT (h)	1320	1546	1750	1955	2220
12 Aug.	θ_s (°)	60	36	25	36	60
	ϕ_s (°)	95	126	180	234	265
	CUT (h)	1335	1552	1746	1946	2203
4 Sep.	θ_s (°)	61	40	33	40	61
	ϕ_s (°)	106	137	180	223	254
	CUT (h)	1351	1558	1743	1929	2135
25 Oct.	θ_s (°)	67	55	52	55	67
	ϕ_s (°)	131	156	180	204	229
	CUT (h)	1429	1509	1728	1847	2028

^aNegative θ_{sp} were arbitrarily assigned for morning times.

Table 4 lists the agronomic data collected for the six dates. The corn canopy had sparse cover on 13 June with better developed row structure two weeks later on 24 June. A period of rapid growth occurred between 24 June and 23 July with canopy cover increasing from 39% to over 90%. Leaf area index quadrupled during this time to its recorded maximum of 4.8. Subsequent dates showed a decrease in LAI and canopy cover but a large increase in total dry phytomass due to grain filling. Finally, by 25 October the canopy was completely senesced with grain at harvest maturity.

The corn had a relatively uniform leaf angle distribution early in the season and tended to become more erect later in the

season (Fig. 2). These results are consistent with those of Pihlman and Ulaby (1981).

Total directional-hemispherical reflectance and transmittance measurements of green corn leaves and tassels were acquired on 17 August with a DK-2 spectrophotometer. Reflectances of corn tassels were much higher than for leaves in all bands with a maximum difference of 75% in the red (Band 3) and a minimum difference of 48% in near-IR (Band 4).

Results and Discussion

The analysis of the spectral data is presented in three parts. The first part considers the effects of projected solar

TABLE 4 Summary of Agronomic Characteristics of Corn Canopies^a

DATE	LEAF AREA INDEX	TOTAL DRY PHYTOMASS g/m ²	CANOPY HEIGHT (cm)	CANOPY COVER (%)	STAGE OF DEVELOPMENT
13 June	0.4 (0.1)	32 (14)	41 (8)	23 (4)	V6 (6 leaves)
24 June	1.2 (0.3)	99 (34)	56 (9)	39 (5)	V8 (8 leaves)
23 July	4.8 (0.4)	804 (155)	261 (21)	96 (2)	VT (tasseling)
12 Aug.	4.4 (0.5)	1637 (290)	280 (9)	94 (1)	R2 (blister)
4 Sep.	4.0 (0.4)	1941 (133)	283 (13)	91 (4)	R5 (dent)
25 Oct. ^b	2.4 (0.2)	—	—	77 (4)	R6 (harvest maturity)

^aStandard deviations are indicated in parentheses.^bBrown leaves only.

angle (θ_{sp}) on reflectance factors viewed at nadir. The second discusses the effects of view angle on reflectance factors at a fixed sun angle. The third section discusses the effects of changing both view and sun angles on reflectance factors of

sparse and fully developed canopies. In the following discussion, the directional notation for reflectance factor (RF) [viz., Eq. (1)] has been omitted for brevity.

Solar angle effects

Figure 3 illustrates the trends of nadir reflectance factors with projected solar angle for the six measurement dates. Considering only the order of the TM bands as the season progressed, we interpret the results in terms of the RF characteristics of the individual scene components. The change in order of near and middle-IR bands from 13 June to 24 June [Fig. 3(a)–(b)] can be explained with the aid of Fig. 4. Note that RF in Band 4 (i.e., near IR) is higher for the fully developed canopy than for soil while Band 7 (i.e., middle IR) RFs are lower (Fig. 4). When LAI increased from 0.4 on 13 June to 1.2

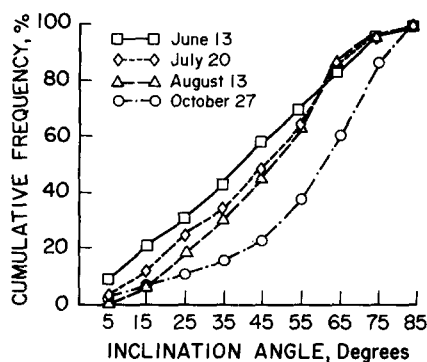


FIGURE 2. Measured cumulative leaf angel distributions for corn canopies on four dates. Leaf inclination angles are midpoints of 10° intervals.

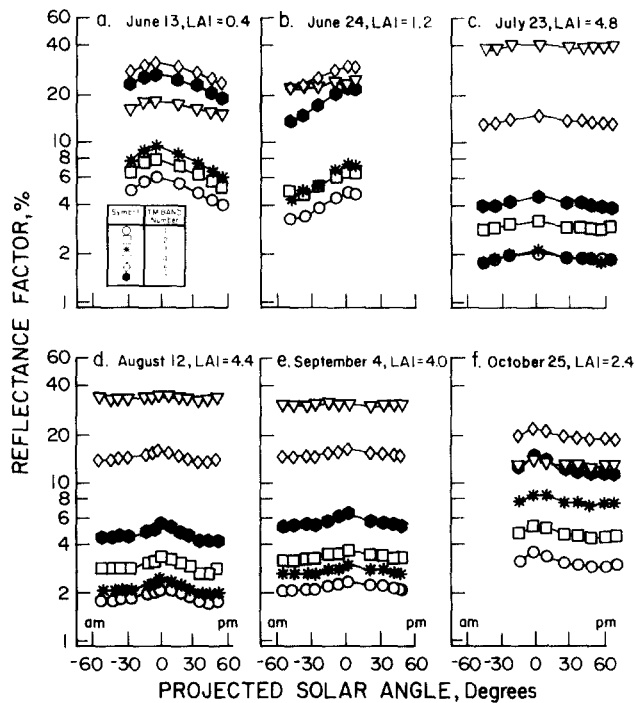


FIGURE 3. Nadir reflectance factors plotted as a function of projected solar angle for corn canopies at six stages of development. Spectral band numbers are noted in legend. Standard deviation are less than or equal to symbol heights.

on 24 June, near-IR RF increased and Band 3 (red) and Band 7 (middle-IR) RFs, decreased indicating an increased amount of vegetation [Fig. 3(a)–(b)]. By 23 July the corn canopy was fully developed and highly reflective in the near-IR band, but less reflective in the visible and middle-IR [Fig. 3(c)]. As the season progressed, the leaves lower in the canopy senesced and green LAI decreased. This is evident in the decreased RF in the near-IR bands and the slight increase in the reflectance of the visible and middle-IR bands [Fig. 3(d)–(e)]. By 25 October the canopy was completely brown with an erectophile leaf arrangement (Fig. 2) as most of the leaves were broken and hanging down. The composite effect of the brown corn leaves and the exposed

bare soil (viz. Fig. 4) resulted in lower near-IR and higher visible and middle-IR RFs [Fig. 3(f)].

With respect to projected solar angle, the RFs tend to decrease for solar angles away from solar noon. Sharp decreases in RF noted for 13 June and 24 June were due principally to increased shadows cast by the plants on the soil surface. Note the change in RF with θ_{sp} for Band 4 on 24 June was not as great as for the other bands [Fig. 3(b)]. This can be attributed to the greater multiple scattering of light by leaves in Band 4 which would tend to fill in shadows cast by the plants (Pinter et al., 1983).

There is a general symmetry about solar noon for RF for closed (> 90% cover) canopies (i.e., 23 July, 12 August, and 4

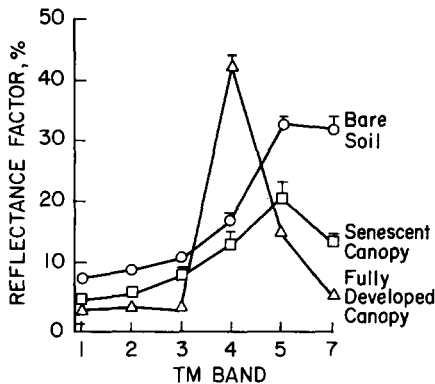


FIGURE 4. Spectral reflectance factors of scene components. Vertical bars indicate plus one standard deviation.

September). Of particular interest are the slight increases in RF that occurred beyond 30° projected solar angle on either side of noon. This phenomenon is probably caused by an increased specular component impinging the nadir viewing sensor at these larger sun angles (Breece and Holmes, 1971; Vanderbilt et al., 1985).

View angle effects

As a sensor is moved from the nadir-viewing position to off-nadir angles, the sides of the canopy come into view and obscure the soil between the plant rows. The effect is to increase the projected foliage area viewed by the sensor. One might expect that, for wavelength bands absorbed by plants, the RF would decrease with view angle. The opposite would be expected for the wavelengths at which plants are strong reflectors of sunlight. Figures 5(a)–(d) present RF data for four different corn canopies for view zenith angles ranging from $\pm 70^\circ$.

The measurements were acquired near solar noon and measured in the plane orthogonal to the sun's principal plane. RFs for negative θ_v were acquired with a

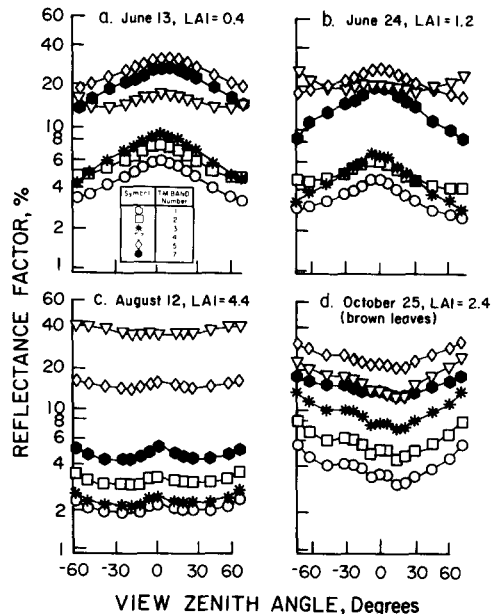


FIGURE 5. Relationship of reflectance factors with view zenith angle for sparse (a and b), fully-developed (c), and senescent (d) corn canopies from data acquired near solar noon. Negative and positive view zenith angles indicate that the radiometer was looking east ($\phi_v = 90^\circ$) and west ($\phi_v = 270^\circ$), respectively. TM spectral band numbers are noted in the legend.

ϕ_v of 90° and RFs with positive θ_v were acquired with $\phi_v = 270^\circ$.

Referring to Figure 5(a), the order of spectral bands for $\theta_v = 0^\circ$ is representative of spectra for bare soil (viz., Fig. 4) which indicates the contribution of the vegetation was small. As the sensor was moved off-nadir on each side of $\theta_v = 0^\circ$, RFs in all bands decreased. At the extreme θ_v , RF in both the near IR (Band 4) and green band (Band 2) increased.

By 24 June [Fig. 5(b)], the increased amount of vegetation was evident by the increasing RF for Band 2 and Band 4 at $\theta_v > 30^\circ$. Note that the order of bands changes from a spectra dominated by bare-soil reflectance at $\theta_v = 0^\circ$ to a spectra dominated by vegetation reflectance at $\theta_v = 70^\circ$.

The effects of the soil background were reduced when the canopy covered most of the soil and different trends of RF with θ_v are apparent for the 12 August data in Fig. 5(c). In this case, the RFs for all bands decreased slightly as the sensor was moved from nadir to about 30° . When θ_v was greater than 30° , RFs increased slightly. For near-nadir views, the FOV included more shaded leaves lower in the canopy so RF was lower. As θ_v increased beyond 30° , mainly the sunlit upper portion of the canopy was viewed and RF increased. In addition, the projected area of highly reflecting tassels increased from 10% at nadir to 24% at $\theta_v = 70^\circ$ and probably contributed to the increases in RF shown in Fig. 5(c).

The corn canopy at harvest maturity on 25 October was characterized by a total lack of green leaves and a complex stand structure caused by many leaning or broken plants. The solar zenith angle was also large with a minimum of 56° at solar noon. RFs in all TM bands were lowest at $\theta_v = 15^\circ$ and increased as θ_v increased. The asymmetry noted in RF for view angles on each side of nadir probably results from a preferred azimuthal position of the leaves. A field survey taken on the day of the RF measurements indicated that a large number of plants were leaning or had tops bending in an easterly direction. Thus the projected area of brown leaves, ears and stalks was greater for the $\phi_v = 90^\circ$ view direction (negative θ_v) and RFs were higher.

Sun and view angle effects

Reflectance factors acquired with view angles of 30° and 60° are presented with view azimuth directions 0° , 90° , 180° , and 270° for a range of sun angles in Figs.

6–8. To minimize confusion, the data are presented as curves which pass through 12–15 individual data points. For the 0° and 180° azimuths, the sensor is pointed parallel to the row direction. For the 90° and 270° azimuths, the sensor views the canopy perpendicular to the rows. A subset of the wavelength bands, TM Bands 3 (red), 4 (near-IR), and 5 (middle-IR), was selected to represent the spectral trends in the data.

The trends of RF with sun angle, view angle, and wavelength for a low LAI canopy (13 June) are illustrated in Figs. 6(a)–(d). Different trends of RF are apparent depending on view zenith and azimuth angle. With the sensor view parallel with the canopy rows ($\theta_v = 0, 180^\circ$) and θ_v at 30° , there was a decrease in RF in all bands for projected

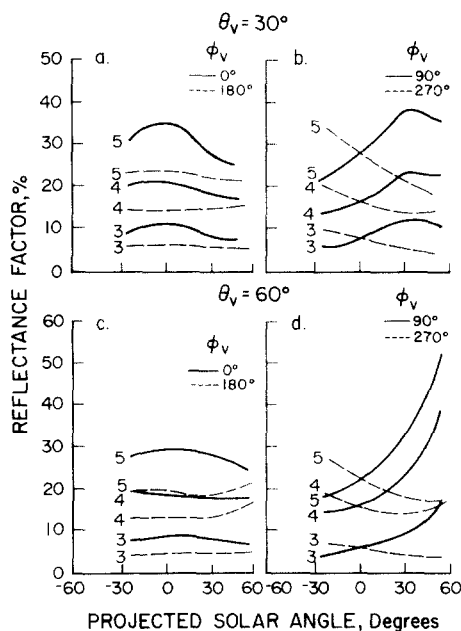


FIGURE 6. Variation in reflectance factors with projected solar angle for a sparse canopy, LAI = 0.4, at different view zenith and azimuth combinations. View zenith (θ_v) and azimuth angles (ϕ_v) are noted above each graph. Spectral band numbers are noted on curves. Data were collected on 13 June 1982.

solar angles away from solar noon [Fig. 6(a)]. However, there was a much higher maximum reflectance for the view direction that was generally away from the sun (i.e., $\phi_v = 0^\circ$). In fact, the sun-view combination where this maximum is reached is quite close to the "hot spot" where the view direction is aligned with the sun. At the hot spot, only sunlit scene components are visible to the sensor. At $(\theta_v, \phi_v) = (30, 180^\circ)$, however, the sensor view direction was generally towards the sun so that shading of leaves was greater than for the opposite view direction $(30, 0^\circ)$. The decline in RF at sun angles before and after solar noon was due to the increased shadowing of the soil between the plant rows.

At $\theta_v = 30^\circ$ and the view direction perpendicular to the rows [Fig. 6(b)], the maximum RF occurred near $\theta_{sp} = 30^\circ$ with the sun generally behind the sensor (i.e., $\phi_v = 270^\circ$). For the opposite view direction ($\phi_v = 90^\circ$), RF decreased with sun angle because of more shaded canopy and shaded soil in the FOV. One might also expect to find a maximum near $\theta_{sp} = -30^\circ$ for the $\phi_v = 90^\circ$ view direction as this angle combination would approach the hot spot for the morning case.

Figures 6(c)–(d) present the data for 60° view zenith angle for the low LAI canopy. Trends were similar to those for $\theta_v = 30^\circ$ except for $(60, 90^\circ)$ where the reflectance maximum occurred near $\theta_{sp} = 60^\circ$. Also, at view position $(60, 180^\circ)$, RFs began increasing for projected solar angles greater than about 30° , which may indicate the presence of first surface reflectance.

The trends of RF for view geometry with projected solar angle for a fully developed canopy are illustrated in Figures 7(a)–(d) with data acquired on 12 August. A relative maximum in RF occurred at

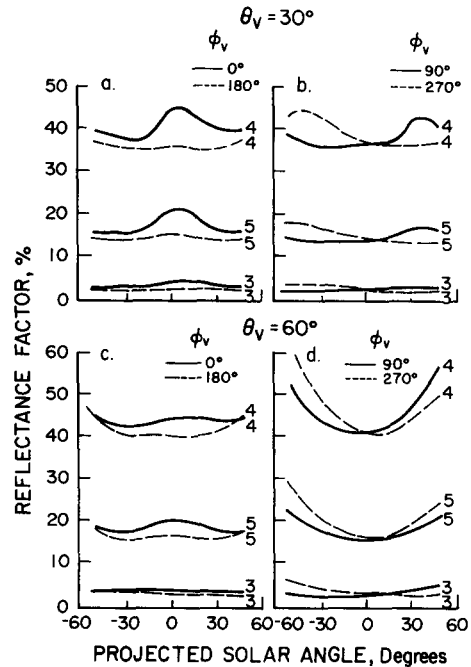


FIGURE 7. Same as Figure 6 except for fully developed canopy, LAI = 4.4. Data were collected on 12 August 1982.

solar noon for view directions parallel to the rows with the 0° view azimuth having greater reflectance than the 180° azimuth at $\theta_v = 30^\circ$ [Fig. 7(a)]. Local reflectance maxima occurred for sun angles away from solar noon for view directions perpendicular to the canopy rows [Fig. 7(b)]. At $\theta_v = 60^\circ$ local reflectance maxima occurred near noon for both $\phi_v = 0$ and 180° in all three bands [Fig. 7(c)]. Away from solar noon RFs decreased and then began to increase as the projected solar angle approached $\pm 60^\circ$. This is again evidence of a first surface or specular reflectance component. In Fig. 7(d), with $\theta_v = 60^\circ$, the reflectance maxima occurred as θ_{sp} approached $\pm 60^\circ$.

Figures 8(a)–(d) demonstrate the diurnal changes in RF for the completely brown canopy. The reflectance maxima for $\phi_v = 0, 180^\circ$ occurred at solar noon for

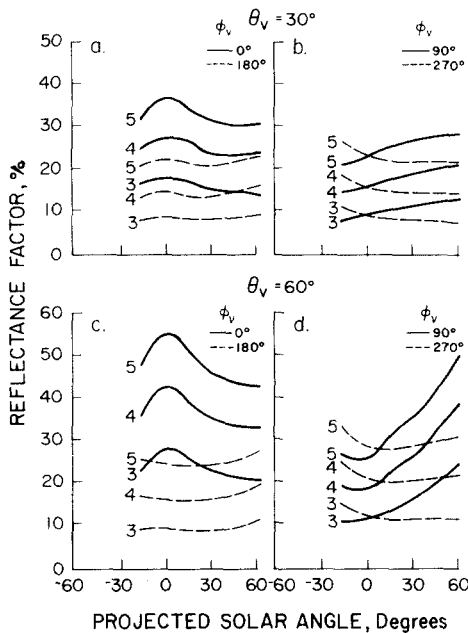


FIGURE 8. Same as Figure 6, except for completely senescent canopy with a brown leaf area index of 2.4. Data were collected on 25 October 1982.

both $\theta_v = 30$ and 60° [Figs. 8(a) and (c)]. The maximum RF values for $\theta_v = 60^\circ$ at $\theta_{sp} = 0^\circ$ in Fig. 8(c) and $\theta_{sp} = 60^\circ$ in Fig. 8(d) were caused by the hot-spot effect mentioned earlier.

For our data, there appears to be a general symmetry of reflectance factors for sun angles on either side of solar noon for the view directions parallel to the rows. The RFs from the view azimuths perpendicular to the rows were asymmetric about solar noon. However, there does appear to be symmetry when the angle between the sun and sensor is considered. For example, RFs for $\phi_v = 90$ and 270° appear to be mirror images as shown in Figs. 7(b) and 7(d). Similar trends are evident from Figs. 7(b) and 7(d) and Figs. 8(b) and 8(d), although the sun angle range is not complete.

The results presented in Figs. 4–8 indicate that the reflectance characteristics of the corn canopies are complex and depend on sun, view, and canopy geometries. For all canopies RF was maximum when the sun and sensor directions coincided. Relative minima occurred for view directions toward the sun.

When the sensor viewing direction was in line with the sun, shadows within the canopy or on the soil surface were hidden by foliage or soil particles. The effect was to maximize the sunlit area of the canopy and soil components projected into the FOV of the sensor. For the view direction 180° from the sun, the probability of viewing shadowed components was maximized, and RF was lowest.

An added source of variation was present for data from low LAI canopies [Figs. 5(a)–(b) and 6]. Here the soil reflectance had an important effect on the composite scene reflectance. The crossover in RF for Bands 4 and 5 was the result of shadows reducing the contrast between the soil and vegetation at the larger sun angles. Near solar noon, however, shadows on the soil were reduced, and the contrast was maximized.

Another factor influencing the trends was the presence of specularly reflected light. This was apparent to the naked eye as shiny spots on the surface of the leaves. The forward scattering noted in the data at larger sun angles was probably due to this specular component. Vanderbilt and Grant (1983) and Vanderbilt et al. (1985) describe specular reflectance from several plant species as well as a technique for estimating its magnitude from measurements of polarized light.

The data presented in this study were collected under essentially cloud-free skies and a very short optical pathlength. Thus

atmospheric effects on the recorded reflectance factors can be assumed to be minimal. To relate the information presented here to high altitude aircraft or satellite multispectral data, the effects of the intervening atmosphere must be included.

Summary and Conclusions

In this study effects of sun and view angles on reflectance factors from corn canopies at various stages of development were examined. For nadir-view angles there was a strong effect of solar zenith angle on RF in all spectral bands for canopies with low LAI. A decrease in contrast between bare soil and vegetation due to shadows as solar zenith angle increased appeared to be the major contributor to this change in RF. Effects of sun angle on reflectance were small for well-developed canopies with high LAI. A moderate increase in reflectance factor was observed at the larger solar zenith angles and was attributed to the presence of specular reflectance.

A strong dependence of reflectance factor and view angle was noted for all of the canopies considered. For canopies with low LAI, reflectance decreased as view zenith angle increased for visible and middle IR wavelength bands which are absorbed by vegetation and RF increased with view angle for multiply scattered near-infrared wavelengths. For higher LAI canopies RFs in the bands considered increased as view zenith angle increased. An increase in RF at large view zenith angles for some view azimuths indicated a specular component in the reflectance data.

Trends of RF with changing sun angle at different view azimuth angles illustrate

that the position of the sensor relative to the sun is an important factor for determining the angular reflectance characteristics of corn canopies. RFs were maximized for coincident sun and view angles and minimized when the sensor view direction was towards the sun. View direction relative to row orientation may also contribute to the variation in RF.

This study represents a step towards understanding the complex relationships between the sun, sensor, and scene for reflectance from crop canopies. The reflectance factor data in concert with the agronomic and physical measurements of the canopies provides a valuable resource for empirical and physically based models of light interactions with vegetation canopies (e.g., Suits, 1972; Cooper et al, 1982; Kimes and Kirchner, 1982; Norman and Welles, 1983; Suits, 1983).

Further studies with these and other similar data sets undoubtedly will yield quantifiable relationships of sun-view angle effects on vegetation reflectance patterns. These data coupled with atmospheric models should also provide significant information towards understanding and exploiting the relationships between sun-view geometry and spectral data for monitoring earth resources from space platforms.

This research was supported by the National Aeronautics and Space Administration under Contract NAS9-16528. Mr. Barrett F. Robinson contributed significantly to the design of the tower system. We wish to acknowledge Purdue students Lois Grant, Dwight Lindman, Jim Meyers, and Bill Severs for their assistance in collecting the data. We also thank Mary Rice for typing the manuscript.

References

- Breece, H. T., III, and Holmes, R. T. (1971), Bidirectional scattering characteristics of healthy green soybean and corn leaves *in vivo*, *Appl. Opt.* 10:119–127.
- Chevrel, M., Courtois, M., and Weill, G. (1981), The SPOT satellite remote sensing mission, *Photogramm. Eng. Remote Sens.* 47:1163–1171.
- Colwell, J. E. (1974), Vegetation canopy reflectance, *Remote Sens.* 3:175–183.
- Cooper, K., Smith, J., and Pitts, D. (1982), Reflectance of a vegetation canopy using the adding method, *Appl. Opt.* 21:4112–4118.
- Eaton, F. D., and Dirmhirn, I. (1979), Reflected irradiance indicatrices of natural surfaces and their effect on albedo, *Appl. Optics* 18:994–1008.
- Guyot, G. (1983), Angular and spatial variability of spectral data in the visible and near infrared, *Proc. Int. Colloq. Spectral Signatures of Objects in Remote Sensing*, Bordeaux, France, 12–16, Sep. pp. 27–44.
- Jackson, R. D. (1984), Remote sensing of vegetation characteristics for farm management, *Proc. SPIE* 465:81–96.
- Kimes, D. S. (1983), Dynamics of directional reflectance factor distributions for vegetation canopies, *Appl. Opt.* 22:1364–1372.
- Kimes, D. S., and Kirchner, J. A. (1982), Radiative transfer model for heterogeneous 3-D scenes, *Appl. Opt.* 21:4119–4129.
- Kimes, D. S., Smith, J. A., and Ranson, K. J. (1980), Vegetation reflectance measurements as a function of solar zenith angle, *Photogram. Eng. Remote Sens.* 46:1563–1573.
- Kirchner, J. A., Kimes, D. S., and McMurtrey, J. E., III (1982), Variation of directional reflectance factors with structural changes of a developing alfalfa canopy, *Appl. Opt.* 21:3766–3774.
- Kollenkark, J. C., Vanderbilt, V. C., Daughtry, C. S. T., and Bauer, M. E. (1982), Influence of solar illumination angle on soybean canopy reflectance, *Appl. Opt.* 21:1179–1184.
- Norman, J. M., and Welles, J. M. (1983), Radiative transfer in an array of canopies, *Agron. J.* 75:481–488.
- Pillman, M., and Ulaby, F. T. (1981), Coherent optical determination of the leaf angle distribution of corn, Univ. Kansas Center for Research, Remote Sensing Laboratory, Lawrence, KS, AgRISTARS Rep. SR-K1-04214, 137 pp.
- Pinter, P. J., Jackson, R. D., Idso, S. B., and Reginato, R. J. (1983), Diurnal patterns of wheat reflectance, *IEEE Trans. Geosci. Remote Sens.* GE-21(2):156–163.
- Ranson, K. J. (1983), A study of the angular reflectance characteristics of corn and soybean canopies, Ph.D. dissertation, Purdue University, West Lafayette, IN, 168 pp.
- Ranson, K. J., Biehl, L. L., and Bauer, M. E. (1985), Variation in spectral response of soybeans with respect to illumination, view and canopy geometry, *Int. J. Remote Sens.* (forthcoming).
- Ritchie, S. W., and Hanway, J. J. (1982), How a corn plant develops, Iowa State Univ. of Science and Technology. Coop. Ext. Serv., Ames, IA, Special Report No. 48, 21 pp.
- Robinson, B. F., and Biehl, L. L. (1979), Calibration procedures for measurement of reflectance factor in remote sensing field research, *Proc. Soc. Photo-Optical Instrumentation Eng.* 23rd Annual Tech. Symp. on Measurements of Optical Radiation, Bellingham, WV, pp. 16–26.
- Schneider, S. R., and McGinnis, D. F. (1982), The NOAA/AVHRR: A new satellite sensor for monitoring crop growth, *Proc. 8th Int. Symp. Machine Processing of Remotely Sensed Data*, LARS/Purdue University, West Lafayette, IN, 7–9 July, pp. 281–290.

- Smith, J. A., Berry, J. K., and Heimes, F. J. (1975), Signature extension for sun angle, Final Report NAS9-14467, Dept. of Earth Resources, Colorado State University, Fort Collins, CO, Vol. I, 101 pp.
- Smith, J. A., Oliver, R. E., and Berry, J. K. (1977), A comparison of two photographic techniques for estimating foliage angle distribution, *Aust. J. Bot.* 25:545-553.
- Suits, G. H. (1972), The calculation of the directional reflectance of a vegetation canopy, *Remote Sens. Environ.* 2:117-125.
- Suits, G. H. (1983), The extension of a uniform canopy reflectance model to include row effects, *Remote Sens. Environ.* 13:113-129.
- Vanderbilt, V. C., and Grant, L. (1983), Light polarization measurements: A method to determine the specular and diffuse light scattering properties of both leaves and plant canopies, Proc. Int. Colloq. on Spectral Signatures of Objects in Remote Sensing, Bordeaux, France, 13-16 Sep.
- Vanderbilt, V. C., Robinson, B. F., Biehl, L. L., Bauer, M. E., and Vanderbilt, A. S. (1980), Simulated response of a multispectral scanner over wheat as a function of wavelength and view-illumination directions, LARS/Purdue University, West Lafayette, IN, LARS Tech. Rep. 071580, 11 pp.
- Vanderbilt, V. C., Grant, L., Biehl, L. L., and Robinson, B. F. (1985), Specular, diffuse and polarized light scattered by two wheat canopies, *Appl. Opt.* (forthcoming).

Received 30 January 1985; revised 5 June 1985.